THE JOURNAL OF PHYSICAL CHEMISTRY B

Article

pubs.acs.org/JPCB

Weak Hydrogen Bonds Formed by Thiol Groups in *N*-Acetyl-L-Cysteine and Their Response to the Crystal Structure Distortion on Increasing Pressure

Vasily S. Minkov*[,†,‡] and Elena V. Boldyreva*[,†,‡]

[†]Novosibirsk State University, 2 Pirogov str., 630090 Novosibirsk, Russian Federation

[‡]Institute of Solid State Chemistry and Mechanochemistry SB RAS, 18 Kutateladze str., 630128 Novosibirsk, Russian Federation

Supporting Information

ABSTRACT: The effect of hydrostatic pressure on single crystals of *N*-acetyl-L-cysteine was followed at multiple pressure points from 10^{-4} to 6.2 GPa with a pressure step of 0.2−0.3 GPa by Raman spectroscopy and X-ray diffraction. Since in the crystals of *N*-acetyl-L-cysteine the thiol group is involved in intermolecular hydrogen bonds not as a donor only (bonds S−H···O) but also as an acceptor (bonds N−H···S), increasing the pressure does not result in phase transitions. This makes a contrast with the polymorphs of L- and DL-cysteine, in which multiple phase transitions are observed already at relatively low hydrostatic pressures and are related to the changes in the conformation of the thiol side chains only weakly bound to the neighboring molecules in the structure and thus easily switching over the weak S−H···O and S−H···S hydrogen bonds. No phase transitions occur in *N*-acetyl-L-cysteine with increasing pressure, and changes in cell parameters and volume vs pressure do not reveal any peculiar features. Nevertheless, a more detailed analysis of the changes in intermolecular distances, in particular, of the geometric parameters of the hydrogen bonds based on X-ray single crystal diffraction analysis, complemented by an equally detailed study of the positions of all the significant bands in Raman spectra, allowed us to study the fine details of subtle changes in the hydrogen bond network. Thus, as pressure increases, a continuous shift of the hydrogen atom of the thiol group from one acceptor (a carboxyl group) to another acceptor (a carbonyl group) is observed. Precise single-crystal X-ray diffraction and polarized Raman spectroscopy structural data reveal the formation of a bifurcated S−H···O hydrogen bond with increasing pressure starting with ∼1.5 GPa. The analysis of the vibrational bands in Raman spectra has shown that different donor and acceptor groups start "feeling" the formation of the bifurcated S−H···O hydrogen bond in different pressure ranges. The results are discussed in relation to some of the previously published data on the effect of high pressure on the polymorphs of L-cysteine, DL-cysteine, and glutathione, that show similarity with the effects reported here for *N*-acetyl-L-cysteine. The results obtained in this work allow one to suggest new models for the pressure-induced structural rearrangements in the whole family of cysteine-containing crystals.

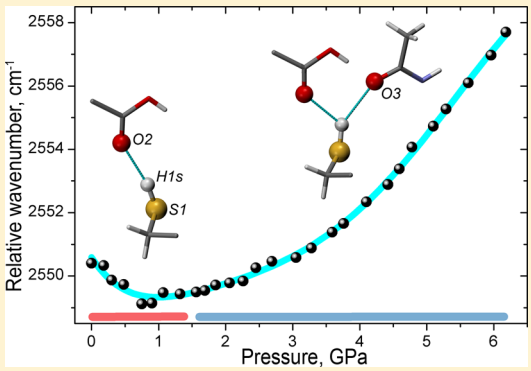

1. INTRODUCTION

High pressure is a powerful tool for studying the properties of hydrogen bonds in various systems. On squeezing, hydrogen bonds can not only shorten but also extend, rotate, and switch over; i.e., the hydrogen atom can shift along the line connecting the non-hydrogen atoms from hydrogen donor to hydrogen acceptor so that the ionization of fragments connected by the H-bond changes (see selected reviews and references therein[1−6]). These phenomena can be accompanied by shifts and rotation of molecular fragments and the whole molecules and result in pronounced macroscopic structural distortions, either preserving the starting phase (anisotropic strain) or inducing its rearrangement (phase transitions).[1−8] Understanding these processes at the microscopic and macroscopic level is important for the theory of phase transitions, polymorphism, crystal engineering, interrelation between stress, strain, and physical or chemical processes in solids. It finds applications in developing new molecular materials, including pharmaceuticals. It is also relevant for understanding dynamic properties and conformational transformations of biopolymers.[9]

N-Acetyl-L-cysteine (NAC) is a compound which is important in several respects and is thus an object of extensive research. It finds important application as a drug for treatment of different diseases and poisonings,[10] including the treatment of paracetamol overdose and metal toxicity, HIV infections, and Alzheimer's and cardiovascular diseases;[11−13] NAC is also boasted as a promising agent in the treatment of psychiatric disorders—addiction, compulsive and grooming disorders, schizophrenia, and bipolar disorder.[14,15] In addition, it is

Received: July 12, 2013
Revised: October 8, 2013

   dx.doi.org/10.1021/jp4068872 | *J. Phys. Chem. B* XXXX, XXX, XXX−XXX

widely used as a mucolytic agent, a potent antioxidant as a scavenger for free radicals produced in cells, and a nutritional supplement as a precursor of cysteine and glutathione. NAC is an important model of interactions in biopolymers and proteins where hydrogen bonds formed by thiol groups of cysteine residues, alongside N−H···O and O−H···O ones, play an essential role in structure formation, for example, of secondary and tertiary structures of proteins having in its crystal structure the −SH group prone to form S−H···O and N−H···S hydrogen bonds.[16−21] Moreover, interactions with participation of a thiol group are crucial for metal binding in the active site of zinc-fingers and iron−sulfur proteins.[22−27]

In a previous publication,[28] we reported that, in contrast to L- or DL-cysteine, NAC does not undergo phase transitions with increasing pressure, and we have interpreted this stabilization with respect to structural transformation in terms of reducing the mobility of the cysteine side chain by the formation of S−H···O and N−H···S hydrogen bonds. *The aim of the present study* was to follow in detail by single-crystal Raman spectroscopy and X-ray diffraction the changes in the different types of hydrogen bonds in the crystal structure vs pressure in relation to the anisotropic lattice strain.

The use of these two techniques in combination has a synergetic effect. Previously, this was illustrated when studying fine details of structural and dynamic changes in the crystals of L-serine,[29] L- and DL-alanine,[30] L- and DL-cysteine,[31,32] some salts based on amino acids and oxalic acids[33] on cooling, as well as in the crystals of DL-alaninium semioxalate monohydrate[34] and sulfamic acid[35] with increasing pressure.

2. EXPERIMENTAL SECTION

Materials. Colorless crystals of NAC were obtained by slow evaporation of a saturated aqueous solution and had a shape of elongated prisms. Crystals of deuterated d_3-NAC were obtained by slow evaporation of saturated solution prepared with D_2O at room temperature. Taking into account the ratio of the integral intensity of modes corresponding to characteristic stretching vibrations of N−H and N−D, as well as S−H and S−D groups, the substitution degree for deuterium was estimated as 88(5)%. (We used a standard procedure for estimating the degree of substitution. Since the polarization of light and the orientation of the crystal are the same, one can calculate the degree of deuteration using the band intensities in the Raman spectrum. In our case, the degree of substitution was estimated as 83% based on the intensities of stretching vibrations S−H/S−D and as 93% based on the pair of N−H/N−D to give the average value as 88% with the error roughly estimated as 5%.) Experiments at high pressures were carried out using good-quality fragments split from the larger crystals with sizes of 0.21 × 0.13 × 0.07 and 0.27 × 0.13 × 0.06 mm^3 for single-crystal Raman spectroscopy and X-ray diffraction, respectively. Hydrostatic pressure was created in a Boehler-Almax type diamond anvil cell equipped with diamonds having low fluorescence, with the diameter of culets equal to 0.60 mm, a stainless steel gasket (starting thickness of 0.200 mm), preindented to 0.095 mm with a drilled hole with about 0.30 mm diameter. A mixture of *n*-pentane and 2-methylbutane (1:1 volume ratio) was used as a hydrostatic pressure fluid. Pressure was estimated from the shift in the R_1-band of a ruby calibrant also loaded into the diamond anvil cell with accuracy of ±0.05 GPa.[36]

Raman Spectroscopy. Raman spectra were measured in the backscattering geometry using a Horiba Jobin Yvon Lab-Ram HR triple-grating spectrometer equipped with an N_2 cooled CCD-2048 × 512 detector Symphony from Jobin Yvon. Excitation was supplied by an argon ion laser (35LAP431 from Melles Griot) with λ = 488 nm and a spectral resolution of 2 cm^{-1}. A Ne-lamp was used for spectral calibration. Raman spectra were measured on increasing pressure in a range from 10^{-4} to 6.18 GPa with a pressure step of 0.2−0.3 GPa and also on reverse decompression.

X-ray Diffraction. Single-crystal X-ray diffraction experiments were carried out using an Oxford Diffraction Gemini Ultra R diffractometer equipped with a molybdenum X-ray tube (λ = 0.71073 Å), a collimator with an outlet diameter of 0.3 mm, and a CCD detector (Ruby from Oxford Diffraction). The diamond anvil cell was aligned with respect to the primary X-ray beam very precisely, so that the difference of the intensities between the position at selected φ, ω, and κ and the opposite position in relation to the primary beam were negligible. The opening angle of the cell is 80° at 2θ, and all reflections beyond this value were rejected. The data collection, indexing, and integration reflections as well as data reduction were performed using CrysAlis software.[37] The Absorb 6.0 software was applied for absorption correction caused by diamond anvils.[38] Crystal structures at all pressures were refined using SHELXL[39,40] integrated in the X-Step32 shell:[41] a structural model refined at the previous pressure point served as the starting point for the subsequent pressure. The Olex-2 software was applied to monitor the quality of the structural model using convenient graphs.[42] Anisotropic displacement parameters of non-hydrogen atoms were restrained with effective standard deviation so their U_{ij} components approximate to more isotropic behavior, although the corresponding isotropic U set was free to vary (ISOR instructions were used to restrain anisotropic thermal parameters of non-hydrogen atoms). H atoms bonded to C, N, S, and O atoms were refined using a riding model, with default distances of methyl C−H = 0.98 Å, secondary C−H = 0.97 Å, tertiary C−H = 0.96 Å, amide N−H = 0.86 Å, hydroxyl O−H = 0.82 Å, and thiol S−H = 1.20 Å with U_{iso}(H) = 1.5 U_{eq} (corresponding parent atom) for the terminal methyl group and U_{iso}(H) = 1.2 U_{eq} for the rest. The methyl group was allowed to rotate around its local 3-fold axes. The parameters characterizing data collection and refinement as well as crystal data are summarized in Table 1. Mercury,[43] CrystalExplorer,[44,45] and PLATON[46] were used for visualization and analysis of the crystal structures. Calculations of principal axes of the anisotropic compression tensor were performed using the PASCal program.[47] The structural data for NAC at 0.52, 1.07, 1.56, 2.12, 2.88, 3.51, 4.42, 5.07, 5.52, and 6.05 GPa are deposited as CIFs at the Cambridge Crystallographic Data Centre (CCDC No. 949292−949301) and also available as Supporting Information; the crystal structure at ambient temperature and pressure is taken from ref 28 with CCDC No. 868554; all the structural data can be downloaded freely from the following site: http://www.ccdc.cam.ac.uk.

3. RESULTS AND DISCUSSION

Crystal Structure and Raman Spectra under Ambient Conditions. NAC crystallizes in the triclinic space group *P*1 with one molecule in the unit cell.[28,48] Like in the case of orthorhombic L-cysteine,[31,49,50] the conformation of the $-CH_2-SH$ side chain is *gauche*+ with the corresponding value of the N1−C2−C1−S1 torsion angle of 61.54(7)° at ambient temperature and pressure. Acylation of L-cysteine leads to the formation of a neutral molecule, while amino acids in crystals exist as zwitterions with ionized ammonium and

dx.doi.org/10.1021/jp4068872 | J. Phys. Chem. B XXXX, XXX, XXX−XXX

Table 1. Crystal Data, Data Collection, and Structure Refinement Parameters for *N*-Acetyl-L-cysteine at Different Pressures[a]

P (GPa)	0.0001[b]	0.52	1.07	1.56	2.12	2.88	3.51	4.42	5.07	5.52	6.05
a (Å)	5.08996(15)	4.9936(8)	4.9311(9)	4.8878(7)	4.8439(8)	4.7987(8)	4.7720(8)	4.7319(9)	4.7062(7)	4.6973(6)	4.6740(8)
b (Å)	5.8843(2)	5.7669(6)	5.6882(6)	5.6295(6)	5.5784(6)	5.5157(7)	5.4738(6)	5.4223(8)	5.3841(6)	5.3706(5)	5.3406(7)
c (Å)	6.5214(2)	6.4314(10)	6.3713(11)	6.3196(9)	6.2771(10)	6.2222(10)	6.1881(10)	6.1428(11)	6.1056(9)	6.0930(8)	6.0654(10)
α (deg)	96.452(3)	96.306(10)	96.240(12)	96.169(10)	96.103(11)	96.077(11)	95.998(11)	95.878(13)	95.840(11)	95.832(9)	95.795(12)
β (deg)	103.859(3)	102.683(13)	101.926(15)	101.376(13)	100.867(13)	100.307(13)	99.989(14)	99.556(15)	99.277(13)	99.131(11)	98.929(14)
γ (deg)	102.076(3)	102.839(11)	103.230(12)	103.500(11)	103.758(12)	103.947(12)	104.110(12)	104.286(15)	104.370(11)	104.403(10)	104.456(12)
V (Å^3)	182.703(11)	173.71(4)	167.91(5)	163.60(4)	159.75(4)	155.33(4)	152.55(4)	148.91(4)	146.27(3)	145.38(3)	143.28(4)
D_{calc} (g cm^{-3})	1.483	1.560	1.614	1.656	1.696	1.745	1.776	1.820	1.853	1.864	1.891
crystal size (mm)	0.41 × 0.19 × 0.13	0.27 × 0.13 × 0.06									
no. of measured,	13790	842	816	807	789	780	775	759	735	718	699
independent, and	4604	423	415	409	402	394	389	383	368	375	354
observed [$I > 2\sigma(I)$] reflections	4192	373	372	369	365	361	365	360	347	353	337
R_{int}	0.0203	0.0402	0.0442	0.0435	0.0422	0.0437	0.0401	0.0412	0.0393	0.0403	0.0398
θ values (deg)	θ_{min} = 3.59	θ_{min} = 3.29	θ_{min} = 3.73	θ_{min} = 3.77	θ_{min} = 3.81	θ_{min} = 3.85	θ_{min} = 3.88	θ_{min} = 3.92	θ_{min} = 3.95	θ_{min} = 3.96	θ_{min} = 3.98
	θ_{max} = 40.24	θ_{max} = 26.36	θ_{max} = 26.37	θ_{max} = 26.35	θ_{max} = 26.23	θ_{max} = 26.35	θ_{max} = 26.27	θ_{max} = 26.36	θ_{max} = 26.31	θ_{max} = 26.34	θ_{max} = 26.18
range of h, k, l	$h = -9 \rightarrow 9$	$h = -5 \rightarrow 5$	$h = -5 \rightarrow 5$	$h = -5 \rightarrow 5$	$h = -4 \rightarrow 4$	$h = -5 \rightarrow 4$	$h = -4 \rightarrow 4$	$h = -4 \rightarrow 4$	$h = -4 \rightarrow 4$	$h = -4 \rightarrow 4$	$h = -4 \rightarrow 4$
	$k = -10 \rightarrow 10$	$k = -7 \rightarrow 7$	$k = -7 \rightarrow 7$	$k = -6 \rightarrow 6$	$k = -6 \rightarrow 6$	$k = -6 \rightarrow 6$	$k = -6 \rightarrow 6$	$k = -6 \rightarrow 6$	$k = -6 \rightarrow 6$	$k = -6 \rightarrow 6$	$k = -6 \rightarrow 6$
	$l = -11 \rightarrow 11$	$l = -6 \rightarrow 6$	$l = -6 \rightarrow 6$	$l = -6 \rightarrow 6$	$l = -6 \rightarrow 6$	$l = -6 \rightarrow 6$	$l = -6 \rightarrow 6$	$l = -6 \rightarrow 6$	$l = -6 \rightarrow 6$	$l = -6 \rightarrow 6$	$l = -6 \rightarrow 6$
R [$F^2 > 2\sigma(F^2)$]	0.0291	0.0339	0.0337	0.0351	0.0324	0.0290	0.0298	0.0310	0.0299	0.0306	0.0291
wR (F^2)	0.0701	0.0725	0.0735	0.0821	0.0708	0.0626	0.0674	0.0707	0.0667	0.0718	0.0643
Flack parameter	−0.06(3)	0.15(16)	−0.22(15)	−0.08(16)	−0.02(15)	0.00(14)	−0.23(14)	−0.23(15)	0.08(15)	−0.25(15)	−0.05(15)
no. of parameters	96	93	93	93	93	93	93	93	93	93	93
no. of restraints	4	57	57	57	57	57	57	57	57	57	57
S	1.040	1.021	1.033	0.999	1.051	1.007	1.043	1.070	1.112	1.051	1.089
$\Delta\rho_{min}$, $\Delta\rho_{max}$ (e Å^{-3})	−0.205, 0.271	−0.099, 0.127	−0.106, 0.132	−0.112, 0.141	−0.107, 0.125	−0.106, 0.111	−0.103, 0.100	−0.125, 0.118	−0.139, 0.112	−0.136, 0.149	−0.144, 0.109

[a]For all structures: chemical formula $C_5H_9NO_3S$, M_r = 163.19, triclinic, $P1$, Z = 1. Experiments were carried out with Mo Kα radiation using an Oxford Diffraction Gemini Ultra R diffractometer. H atoms treated by constrained refinement. [b]The data taken from ref 28 with CCDC No. 868554.

dx.doi.org/10.1021/jp4068872 | J. Phys. Chem. B XXXX, XXX, XXX−XXX

carboxyl groups.[51] Thus, the molecule of NAC has three different fragments, namely, thiol, carboxyl, and amide, which all can act as donors for hydrogen bonds in the crystal structure. Two carbonyl groups (one from amide, another form carboxyl) may serve as acceptors for hydrogen bonding. As a result, in the crystal structure of NAC, there are three different types of hydrogen bonds (S−H···O, O−H···O, and N−H···S); each of them forms infinite chains expanding in different crystallographic directions, forming a three-dimensional hydrogen bonded framework. Several projections of the crystal structure are shown in Figure 1. A short O−H···O hydrogen bond

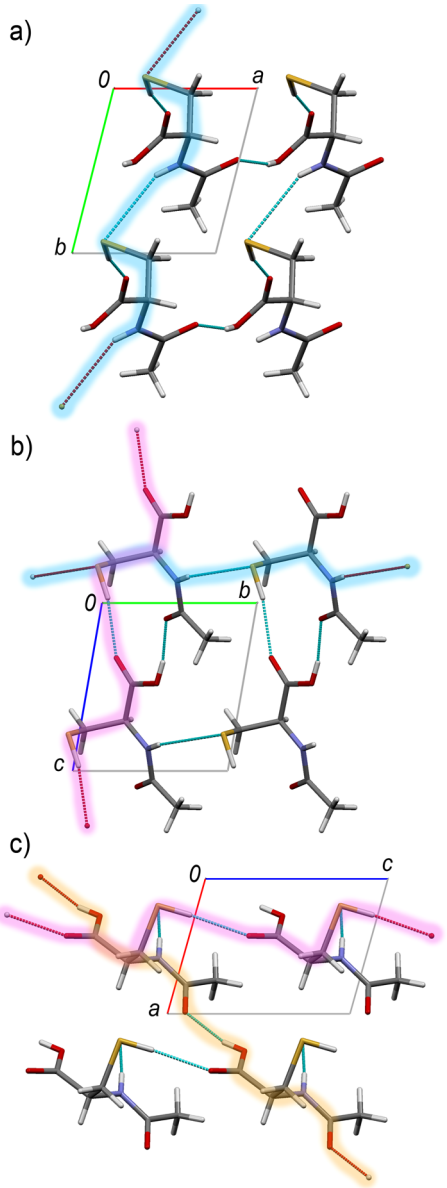

Figure 1. The fragments of the crystal structure of *N*-acetyl-L-cysteine at ambient temperature and pressure viewed in different orientations. The infinite chains formed by O−H···O, S−H···O, and N−H···S hydrogen bonds are highlighted by color.

formed by carboxyl and carbonyl groups with the O···O distance of 2.5758(8) Å gives rise to infinite chains of C(7) type expanding along the [101] crystallographic direction (for more details about graph sets, see ref 52). The infinite chains of C(6) type built up by the S−H···O hydrogen bond extend along the *c* crystallographic axis linking the side chain and the carboxyl group of another molecule together. In contrast to the crystals of monoclinic and orthorhombic L-cysteine as well as of DL-cysteine where the thiol group forms predominantly S−H···S hydrogen bonds, the side chain in the structure of NAC forms a S−H···O hydrogen bond with a S···O distance of 3.4699(7) Å, which is a little longer than in monoclinic (3.404(1) Å)[53] and orthorhombic (3.3812(13) Å)[31] L-cysteine but shorter than it is in the low-temperature/high-pressure polymorph of DL-cysteine (3.609(3) Å).[32,54] A very interesting feature of the structure is the presence of N−H···S hydrogen bonds with a N···S distance of 3.7519(6) Å. The analysis of the 42 contacts of the N−H group with the thiol S-atom present in 36 different crystal structures deposited in the CSD up to now (version 5.34)[55] reveals an average N···S distance of 3.72(6) Å, which is quite close to the value in NAC. This distance is significantly longer than the N···O distance in the corresponding N−H···O hydrogen bonds found in α-amino acids;[56] in some respect, this is due to the larger van der Waals radius of the sulfur atom, though the difference in N···X length exceeds the difference between van der Waals radii of O and S atoms.[57] The analysis of the 35 L- and DL-crystal structures of natural α-amino acids found in the CSD shows that the refined average N···O distance is equal to 2.831(5) Å. The infinite chains of C(5) type formed by N−H···S hydrogen bonds stretch along the crystallographic axis *b*.

Very important information about intermolecular interactions can be obtained from Raman spectra (Figure 2). In order to make a more accurate assignment, an additional measurement was performed using a partially deuterated sample, d_3-NAC. Observed Raman bands and their assignment are summarized in Table 2. In the Raman spectrum of NAC, stretching vibrations of S−H and S−D were observed at 2550 and 1857 cm^{-1}, respectively. In both cases, bands were narrow, very intensive, and had no shoulders, which gives evidence of ordering of the thiol groups in the structure. In contrast to that, in the crystals of the monoclinic and orthorhombic polymorphs of L-cysteine, the thiol groups are disodered and are involved in the formation of S−H···O and S−H···S hydrogen bonds;[31,53,58] subtle disordering was also observed in the crystals of DL-cysteine.[32] Despite the variation of S···O distance in the three crystal structures, the $(S-H)_{str}$ bands characterizing the −SH groups involved in S−H···O hydrogen bonds are found in all the cases in a quite narrow range 2545−2552 cm^{-1}. In the Raman spectrum, an intensive and narrow band at 3377 cm^{-1} corresponds to the stretching vibrations of the N−H group, while for the crystals of L- and DL-cysteine this vibration is either not observed at all or manifests itself as a weak and broadened band.[31,32,58−60] (There is no unambiguous relation between the intensities of the N−H and O−H stretching vibrations in Raman spectra and their involvement in H-bonding. The result is usually an interplay of the effects of H-bond strength itself and of the disordering of the group. At the same time, such a correlation seems to exist for the width of the Raman stretching band: the greater the half-width, the stronger H-bonding (very often there is a very large band broadening, especially for O−H stretching vibration even on cooling). In the crystals of amino acids, N−H and O−H vibration bands have very low intensities, and cysteine is not an exception. Acylation gives a neutral molecule instead of the zwitterions, and this affects the H-bonding considerably, which, as well as the formation of the weak N−H···S hydrogen bond, can account for a significant change in the intensity and the width of the NH vibration.) In orthorhombic L-cysteine, the

dx.doi.org/10.1021/jp4068872 | J. Phys. Chem. B XXXX, XXX, XXX−XXX

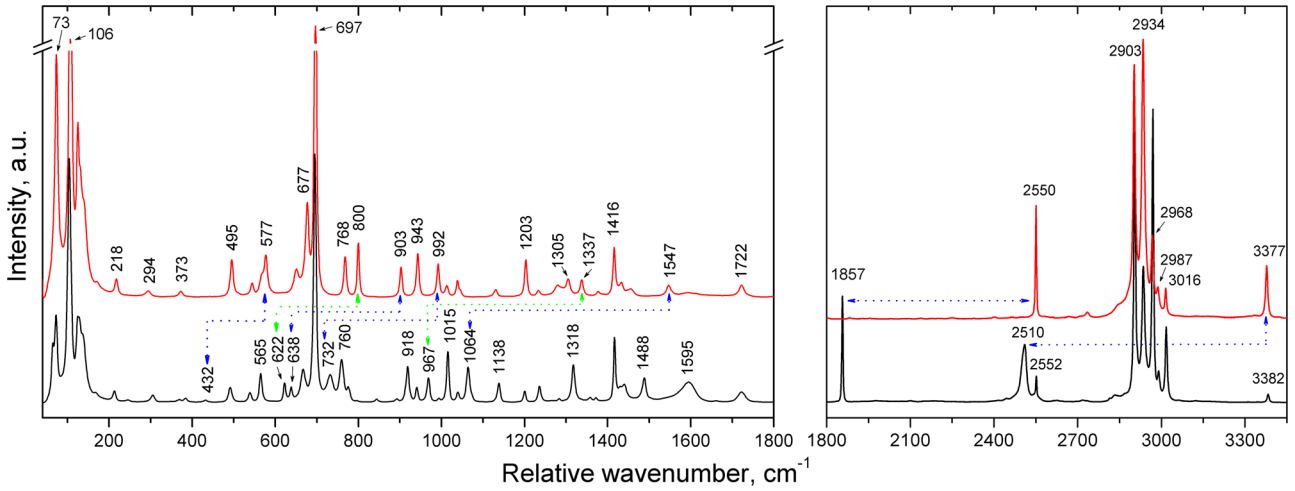

Figure 2. Raman spectra of *N*-acetyl-L-cysteine (top) and its deuterated analogue d_3-*N*-acetyl-L-cysteine (bottom). The shift to the low-wavenumber region of some bands caused by deuteration is highlighted by dotted lines.

$(N-H)_{str}$ vibrations were observed at 3162 cm^{-1} in the FTIR spectrum;[60] later, they were assigned to the vibrations of the N−H groups involved in the longest N−H···O hydrogen bond in the structure (with the corresponding N···O distance equal to 3.0222(18) Å).[31] In racemic DL-cysteine, only a weak shoulder was present at ∼3150 cm^{-1}. The observed wavenumbers of the $(N-H)_{str}$ vibrations are in good agreement with the structural data: N−H···O hydrogen bonds in the racemic form are shorter than those in the chiral one.[60] Thus, both a longer N···S distance and a higher wavenumber of the $(N-H)_{str}$ mode indicate the considerably weaker N−H···S hydrogen bonds in NAC as compared to the N−H···O hydrogen bonds in L- and DL-cysteine. The mode of $(N-D)_{str}$ stretching vibrations is observed at 2510 cm^{-1}, but it is broadened (the mode halfwidth is doubled as compared to that of N−H) and has a shoulder at ∼2502 cm^{-1}, indicating disordering of the amide group in a crystal of d_3-NAC, probably because of incomplete deuteration. In the Raman spectrum of d_3-NAC, a new band with a moderate intensity appears at 1488 cm^{-1}; most likely, this band corresponds to $(O-D)_{str}$. Unfortunately the O−H stretching vibrations are not clearly revealed in unpolarized Raman spectra; however, the polarized spectra at low temperatures showed the presence of a weak, composite, and broadened band at ∼1990 cm^{-1}, which, considering that O−H···O hydrogen bonds are strong, could be assigned to $(O-H)_{str}$. Such a low wavenumber is characteristic for strong O−H···O hydrogen bonds with typical $(O-H)_{str}$ values observed in the range 800−2500 cm^{-1}.[61] Band nos. 2−6 in the spectral region of 2900−3000 cm^{-1} are related to the stretching vibrations of the C−H and CH_2 groups.

The spectral range of 1750−1200 cm^{-1} is mainly represented by stretching vibrations of C═O and COOH groups and bending vibrations of N—H, C—H, and CH_2. The band at 1722 cm^{-1} can be assigned to stretching vibrations of the carbonyl C═O groups, though its wavenumber is higher than one would expect for a carbonyl group involved in strong hydrogen bonds (anticipated at 1630−1680 cm^{-1}). The next two weak and broadened bands with maxima at ∼1593 and 1547 cm^{-1} correspond to the asymmetrical stretching vibrations of COOH and bending vibrations of N—H, respectively. The intensity of the first band strongly depends on the polarization of the Raman spectra and remains the same after deuteration, while the second one disappears on deuteration, and the bending vibrations of N—D manifest themselves at 1064 cm^{-1}. Several bands in the range of 1370−1280 cm^{-1} can be assigned to symmetrical stretching vibrations of the carboxyl group and the mixed vibrations of carbonyl $(C═O)_{str}$, $(C—N)_{str}$, and $(N—H)_{bend}$ groups, also known as amide-III. Bands of this region changed considerably with deuteration: two bands at 1337 and 1305 cm^{-1} having moderate intensity turned to very weak shoulders of a strong band at 1318 cm^{-1} that appeared in the Raman spectrum of d_3-NAC together with the weak one at 1358 cm^{-1}. At the same time, the band at 967 cm^{-1} that appeared in the spectrum of the deuterated sample confirms the contribution of $(N—H)_{bend}$ to these composite vibrations represented by mode nos. 17−20. Several bands at 1416, 1433, and 1456 cm^{-1} can be assigned to planar bending vibrations of C—H and CH_2, whereas those at 1233, 1203, and 1131 cm^{-1}, to out-of-plane bending vibrations of the same groups, since their positions are not sensitive to the deuteration.

The range of the low wavenumbers is less informative. Nevertheless, some bands could also be characterized. Taking into account both the results of previously published works[31,32,58−60,62−70] devoted to FTIR and Raman spectroscopic investigations of cysteine and the loss of the band intensity after deuteration observed in this work, the band at 992 cm^{-1} should be assigned to bending vibrations of the thiol group. The corresponding $(S-D)_{bend}$ band in the Raman spectra of d_3-NAC was observed at 732 cm^{-1}. The strong band at 918 cm^{-1} that appeared in the Raman spectrum of the deuterated sample might also be assigned to the composite vibration nos. 17−20 (as the band at 967 cm^{-1}) but can also correspond to the $(O-D)_{bend}$ mode. Two strong bands at 800 and 903 cm^{-1} significantly lose their intensities, and two bands appear at 622 and 638 cm^{-1} in the spectra of the deuterated sample. They may be associated with the vibrations of those molecular groups which are affected by deuteration. Most likely, the band at 800 cm^{-1} (and the corresponding band at 622 cm^{-1}) is related to the out-of-plane bending vibrations of N−H (N−D), though the expected wavenumber for these vibrations in a secondary amide is somewhat lower.[71] The band at 768 cm^{-1} is probably assigned to the $(COOH)_{bend}$ mode. The strong band at 697 cm^{-1} corresponds to the $(C-S)_{str}$ vibration, and its position is comparable with those observed in the Raman spectra of the crystals of L- and DL-cysteine.[31,32,58−60] The spectral range below 600 cm^{-1} is very difficult for band assignment. It is characterized

dx.doi.org/10.1021/jp4068872 | J. Phys. Chem. B XXXX, XXX, XXX−XXX

Table 2. Observed Raman Bands and Their Assignment in the Raman Spectra of the Deuterated d_3-*N*-Acetyl-L-cysteine under Ambient Conditions and of *N*-Acetyl-L-cysteine at Different Pressures[a]

		d_3-NAC	NAC			
band number	assignment	ambient conditions		2.06 GPa	4.10 GPa	6.18 GPa
1	NH_{str}/ND_{str}	3382/2510 m	3377 m	3339	3315	3299
2	$CH_{2\ str}$ CH_{str}	3017	3016 w	3044	3066 + 3054	3087 + 3070
3	$CH_{2\ str}$ CH_{str}	2990	2987 w	3001 sh		
4	$CH_{2\ str}$ CH_{str}	2969	2968 m	2993	3011	3026 + 3029 sh
5	$CH_{2\ str}$ CH_{str}	2935	2934 s	2943	2951	2960
6	$CH_{2\ str}$ CH_{str}	2905	2903 s + 2885 sh	2921 + 2896 w	2936 + 2906	2953 + 2916
7	SH_{str}/SD_{str}	2552/1857 s	2550 s	2549	2552	2558
8	OH_{str}/OD_{str}	1488 m	~1990 w	~1925	~1875	
9	$C{=}O_{str}$	1722	~1722 m	1705	1701	1702
10	CO_2H_{str}	1595	~1593 w	~1510		
11	NH_{bend}/ND_{bend}	1064 s	1547 m	1559	1574	1590
12	$CH_{2\ bend}$	1440	1456 sh	1454	1457	1461
13	$CH_{2\ bend}$	1430	1433 sh			
14	$CH_{2\ bend}$	1417	1416 s	1416	1419	1424
15		1372	1377 w	1378	1382	1389
16		1358 w				
17	$C{=}O_{str}$ + CN_{str} + NH_{bend}/ND_{bend}	1335 sh/967 m	1337 m			
18	$C{=}O_{str}$ + CN_{str} + NH_{bend}/ND_{bend}	1300 sh	1305 m	1300 sh	1303	1307
19	$C{=}O_{str}$ + CN_{str} + NH_{bend}/ND_{bend}	1318 s				
20	$C{=}O_{str}$ + CN_{str} + NH_{bend}/ND_{bend}	1284	1279 sh	1278	1276	1281
21	$CH_{2\ wagg}$	1236	1233 w	1237	1243	1248 + 1225
22	$CH_{2\ wagg}$	1200	1203 s	1203		
23		1138	1131 w	1133	1135	1135
24		1040	1039 m + 1045 sh	1038 + 1055	1041 + 1064	1045 + 1075
25		1015	1013 m	1018	1021 sh	
26	SH_{bend}/SD_{bend}	994 w/732	992 s	1000	1008	1017
27		940	943 s	955	965	976
28	OD_{bend}?	918 s				
29		892/638 w	903 s	918	928	939
30		844 w				
31	NH_{rock}/ND_{rock}?	796/622 w	800 s	817	833	847
32	$COOH_{wagg}$	760 + 776 sh	768 s	779	788	797
33	CS_{str}	696	697 s	713	728	741
34		667	677 m + 650 w	694 + 660	708 + 670 w	723 + 681 w
35		432 w	577 m	591	596 + 605	601 + 615
36		565	568 sh			
37	CCN_{bend} CCC_{bend} CCS_{bend}	539	544 w	547	550	555
38	CCN_{bend} CCC_{bend} CCS_{bend}	492	495 m	490	492	496
39	CCN_{bend} CCC_{bend} CCS_{bend}	384 w				
40	CCN_{bend} CCC_{bend} CCS_{bend}	369	373 w	382 + 402	389 + 422	394 + 447
41	CCN_{bend} CCC_{bend} CCS_{bend}	305	294 w	304	315	327
42		245 w				
43		213	218 w	231	244	257
44	region of lattice modes	167	170 sh	181	193 + 207 sh	203 + 230
45	region of lattice modes	137	139 sh			
46	region of lattice modes	128	130 sh	156	176	194 sh
47	region of lattice modes	125	125 m	140	157	174
48	region of lattice modes	104	106 s	132	146	156 + 162
49	region of lattice modes	72 + 65 sh	73 s	84 + 96	98 + 110	109 + 123

[a]Intensities of bands are labeled as w - weak, m - medium, s - strong, sh - shoulder.

by lattice modes and by different torsion vibrations of CCC, CCN, CCS, and SH. The most substantial difference between the two Raman spectra is the disappearance of the band at 577 cm^{-1} for NAC and the appearance of the band at 432 cm^{-1} for its deuterated analogue.

Crystal Structures and Raman Spectra at High Pressures. On increasing pressure, the cell parameters and volume change continuously without any hint of a phase transition (Figure 3). No evident hysteresis on subsequent decompression was observed. The most compressible parameter is *b*; its relative change when pressure reaches 6.05 GPa is −9.240(15)%. The largest parameter *c* shows the smallest change of −6.992(18)%, and the relative compression of *a* is 8.172(18)%. Changes in the triclinic α, β, and γ angles are not

dx.doi.org/10.1021/jp4068872 | J. Phys. Chem. B XXXX, XXX, XXX−XXX

the same: the α angle has a little change of −0.681(16)%, whereas the β angle decreases at 4.747(16)% and the γ angle increases to 2.332(15)%. The changes of the cell parameters and volume are not exactly the same for all three data sets obtained from powder[28] and single-crystal X-ray diffraction experiments using different pressure-transmitting liquids. The cell parameters and volume refined from powder patterns obtained with fluorinert as a pressure-transmitting fluid (black figures in Figure 3) are systematically larger as compared to those refined from single crystals immersed in pentane/isopentane mixture at the same pressure. Moreover, the difference between two single crystal data sets obtained using different pressure-transmitting fluids is quite significant: although the changes in the value of the *a* parameter are similar, the *b* and *c* parameters decrease less in the experiment with fluorinert as a hydrostatic media than in the other one with pentane/isopentane mixture. Thus, the measured compressibility of the structure of NAC is different when different hydrostatic pressure transmitting media are applied. The most probable reason of this phenomenon could be not absolutely hydrostatic compression when using fluorinert.[72] Earlier, it was described that the choice of a pressure-transmitting liquid may be critical also for the occurrence or non-occurrence of a phase transition, as well as for the fragmentation or preserving the crystal intact at high pressure.[73−76]

Since the crystal structure of NAC is triclinic, the principal axes of the anisotropic compression tensor do not coincide with the main crystallographic directions [100], [010], and [001]. The relative linear strain along the principal axes of the tensor is shown in Figure 4, as well as the direction of the principal axes with respect to the crystal structure. The compressibility along different principal strain directions differs more as compared with the difference in compressibility along the *a*, *b*, and *c* crystallographic axes. The major compression (in the 3P direction) is about 4.7 times larger as compared to the minimum compression (in the 1P direction). The "3P direction" (with relative compression of −12.30% at 6.05 GPa) does not correspond to the direction of any hydrogen bonds in the structure. It is clearly shown in Figure 4b that this direction is almost perpendicular to all the types of hydrogen bonds. The "2P direction" (relative change −8.42%) mostly coincides with the directions of S−H···O and N−H···S hydrogen bonds. The relative changes in the lengths of these hydrogen bonds correlate with the changes in the *b* and *c* crystallographic parameters, along which the infinite chains formed by these bonds stretch: the relative shortening of the S−H···O and N−H···S hydrogen bonds is −6.80(16) and −9.27(12)%, respectively. The direction of the least compression ("1P direction") (−2.61% at 6.05 GPa) matches with the direction of strong O−H···O hydrogen bonds.

The conformation of an NAC molecule is very rigid and does not undergo significant changes on increasing pressure. The $-CH_2SH$ side chain preserves the *gauche*$^+$ conformation, and the values of the corresponding N1−C2−C1−S1 and C3−C2−C1−S1 torsion angles have a slight variation in the whole pressure range near 62 and −62.5°, respectively. Small changes are observed for the carboxyl group which slightly rotates along the C2−C3 bond (the corresponding C1−C2−C3−O1 torsion angle decreases from 124.63(7)° at ambient pressure to 117.9(12)° at 6.05 GPa) and for the methyl group which moves out of the almost planar skeleton of the molecule C2−N1−C4−O3 (the corresponding C5−C4−N1−C2 torsion angle decreases from 178.05(7)° at ambient pressure to 175.1(11)° at the highest pressure).

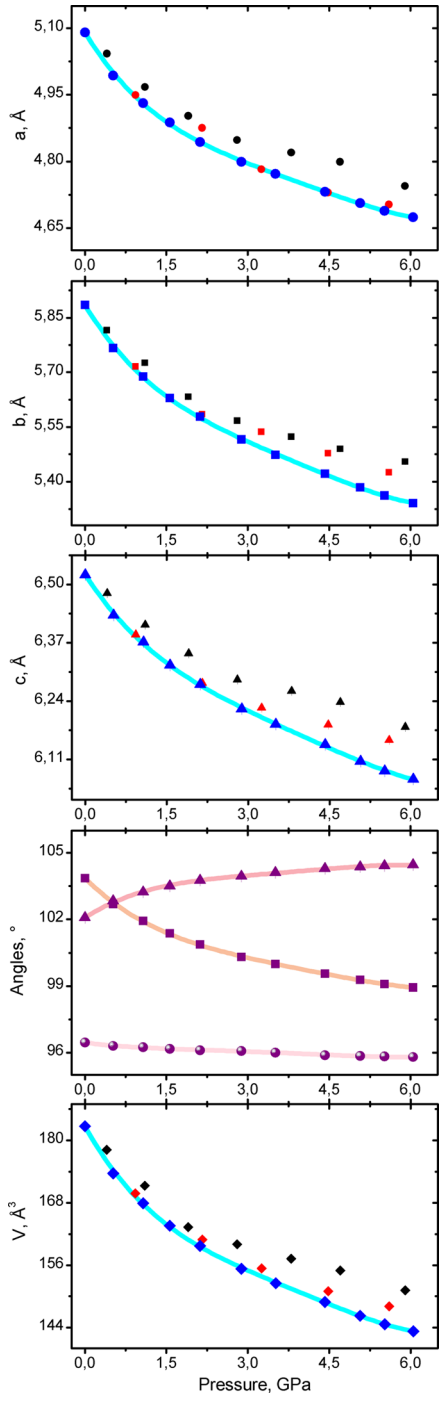

Figure 3. Cell parameters and volume in *N*-acetyl-L-cysteine on increasing pressure: blue symbols are used for the *a*, *b*, and *c* cell parameters and volume measured in the single-crystal X-ray diffraction experiments using pentane−isopentane as a pressure-transmitting fluid. For a comparison, black and red symbols are used for data refined from powder data[28] (black) and from an additional single-crystal X-ray diffraction experiment using fluorinert as a hydrostatic pressure transmitting media (red). The values for the triclinic angles α, β, and γ (purple circles, squares, triangles, respectively) are plotted for data retrieved from single crystal X-ray diffraction using a mixture of pentane and isopentane. The standard deviations of each value calculated in a standard way for a single experiment are less than the size of symbols, but data dispersion for different samples (powder, single crystal) and experiments using different pressure-transmitting fluids is apparently larger. All curves are guides to the eye.

dx.doi.org/10.1021/jp4068872 | J. Phys. Chem. B XXXX, XXX, XXX−XXX

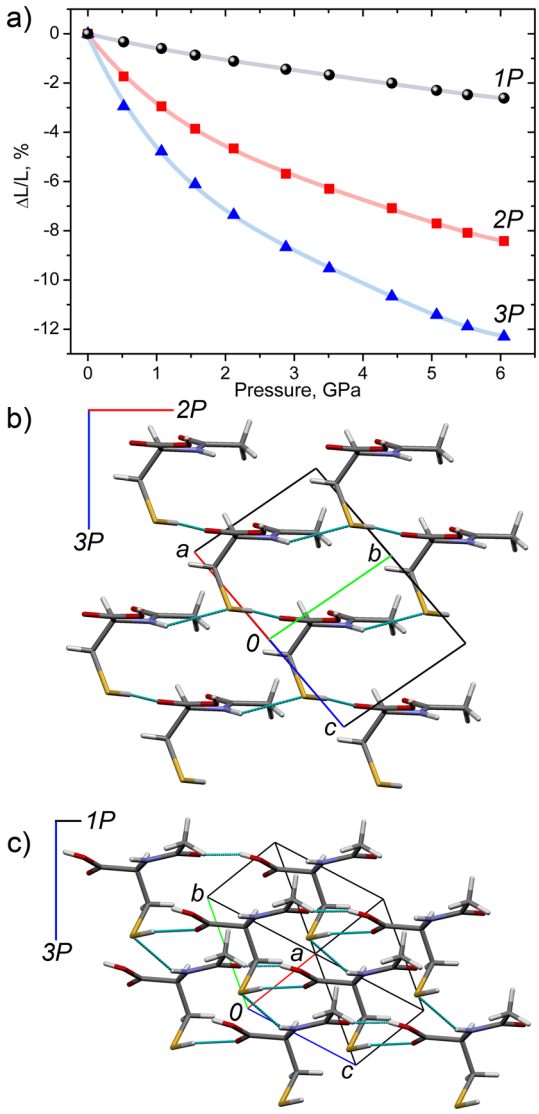

Figure 4. (a) The relative linear strain along the principal axes of the tensor with labeling. All curves are guides to the eye. (b and c) Projections of the *N*-acetyl-L-cysteine crystal structure and directions of the principal tensor axis (labeling and color correspond to part a).

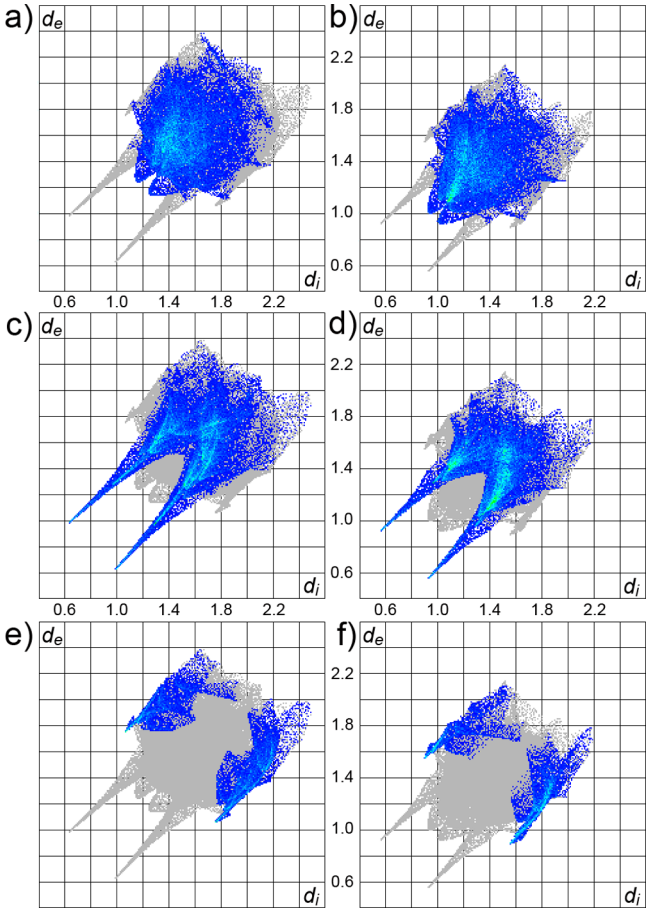

Figure 5. Two-dimensional fingerprint plots for *N*-acetyl-L-cysteine at ambient pressure (a, c, e) and at 6.05 GPa (b, d, f), showing the H···H contacts (a and b), the O···H contacts (c and d), and the S···H contacts (e and f) in colored areas (including reciprocal contacts) but keeping the rest of the interactions present in the crystal structure in gray. See about the fingerprint plots in refs 44, 45, and 77.

Compression of the crystal structure on increasing pressure leads to the changes of intermolecular interactions. Due to the diminishing voids in the crystal structure, long intermolecular contacts disappear: there are no contacts longer than 4 Å in the structure at 6.05 GPa. The "fingerprint plots" describing intermolecular interactions in the crystal at the ambient pressure and 6.05 GPa are plotted in Figure 5. On increasing pressure, the contribution of the H···H interaction remains the same (38.6% at ambient pressure and 38.9% at 6.05 GPa), but the nature of these contacts changes. Under ambient conditions, the short and medium H···H contacts correspond to the interaction between the methyl group from an acetyl fragment and the methylene group from the —CH_2—SH side chain of the neighboring NAC molecule. At high pressures, this area is mainly represented by the contacts of the thiol group with the methylene and methyl groups. The contribution of the O···H contacts also does not change (39.3% at ambient and 38.8% at 6.05 GPa); the narrow area is related to short O—H···O hydrogen bonds in the structure which get even shorter with increasing pressure. The fingerprint plot of these contacts at ambient pressure (Figure 5c) has two intersecting areas highlighted sky blue color in the region of medium contacts. The first one with a shorter O···H distance of ∼2.8−3.0 Å is related to the contacts with the participation of the C═O from a carboxyl group. The second one with a longer O···H distance of ∼3.1−3.2 Å corresponds to the contacts with the carbonyl at the amide group. At 6.05 GPa, two areas are merged into one with an average O···H distance of ∼2.5−2.7 Å; thus, two carbonyl oxygen atoms are involved in the formation of O···H contacts with a similar O···H distance. For these interactions, hydrogen comes mainly from the thiol, methylene, and methyl groups. The contribution of the S···H contacts is reduced from 15.0% at ambient pressure to 11.9% at 6.05 GPa; the narrow area characterizing short contacts corresponds to the N—H···S hydrogen bonds, which become stronger with increasing pressure; while the amount of long contacts related to different C—H···S interactions and presented by broad and quite distributed area significantly reduces with pressure.

The changes in the crystal structure induced by increasing pressure manifest themselves also in Raman spectra. Figure 6a shows Raman spectra of NAC at several pressures. The data on the bands observed in Raman spectra at 2.06, 4.10, and 6.18 GPa are summarized in Table 2. Shifts of the positions of the

dx.doi.org/10.1021/jp4068872 | J. Phys. Chem. B XXXX, XXX, XXX−XXX

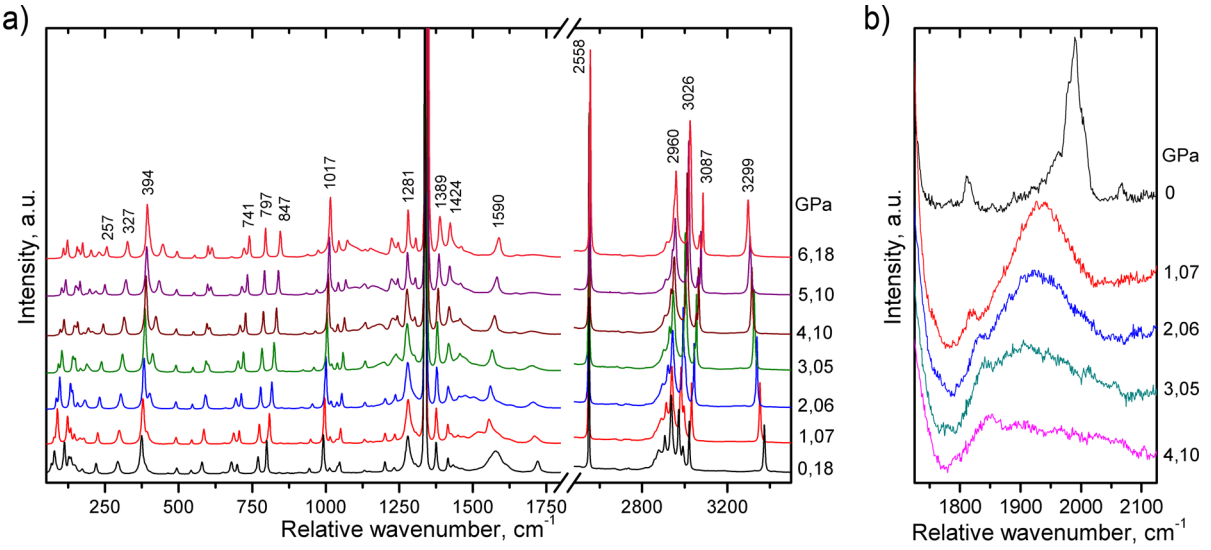

Figure 6. (a) Raman spectra of *N*-acetyl-L-cysteine at several pressures; (b) enlarged region of the $(O-H)_{str}$ band in Raman spectra at different pressures. The change in the relative intensity of the bands in Raman spectra taken at high pressures in a DAC as compared to those at ambient pressure for another, "free" crystal (Figure 2) (see, e.g., the C−S stretching band) is related to the different orientations of the samples and a strong dependence of the intensities of some bands on the orientation, as well as to the effect of diamonds on the polarization of light.

Table 3. The Geometry of Hydrogen Bonds (the D···A Distance, Å, and the D−H···A angle, deg) in the Crystal Structure of *N*-Acetyl-L-cysteine at Different Pressures

pressure (GPa)	O1−H1o···O3		N1−H1n···S1		S1−H1s···O2		S1−H1s···O3	
0.0001	2.5758(8)	163.0	3.7519(6)	153.5	3.4699(7)	169.0	3.8885(8)	119.5
0.52	2.562(6)	157.8	3.674(4)	151.9	3.439(6)	136.9	3.829(6)	143.7
1.07	2.556(7)	159.5	3.620(4)	151.1	3.414(6)	142.1	3.781(6)	134.5
1.56	2.533(7)	159.9	3.579(4)	153.8	3.384(6)	133.4	3.746(6)	145.7
2.12	2.532(7)	161.5	3.547(4)	152.5	3.361(6)	129.1	3.709(6)	150.1
2.88	2.515(6)	168.8	3.508(3)	153.0	3.329(5)	129.2	3.671(5)	148.2
3.51	2.500(6)	168.7	3.486(4)	152.5	3.319(5)	126.4	3.640(5)	151.6
4.42	2.491(7)	168.6	3.452(4)	154.6	3.285(5)	129.9	3.609(6)	144.8
5.07	2.480(7)	168.3	3.428(4)	153.8	3.264(5)	127.3	3.578(6)	148.4
5.52	2.474(7)	169.6	3.420(4)	154.7	3.256(5)	127.2	3.564(6)	148.0
6.05	2.462(6)	169.2	3.404(4)	156.0	3.234(5)	128.0	3.546(5)	146.3

Raman bands on increasing pressure were continuous without any jump-wise changes, thus confirming the previously reported data on the absence of any phase transitions.[28]

The stretching vibrations of hydrogen-bonded O−H and N−H groups shifted significantly to the low-wavenumber range in agreement with the strengthening of O−H···O and N−H···S hydrogen bonds. The broad band of $(O-H)_{str}$ has a red shift of more than 100 cm^{-1} on increasing pressure to 4.10 GPa (Figure 6b); after having reached this pressure, the band became poorly detectable due to low intensity. At 6.05 GPa, the O···O distance in the O−H···O hydrogen bond reached a very short value of 2.462(6) Å (Table 3). The relation between the $(O-H)_{str}$ wavenumber and the O···O distance is in a good agreement with the "Novak correlation" and may be classified as a strong hydrogen bond.[61] The change of the $(COOH)_{str}$ band on increasing pressure confirms the strengthening of hydrogen bonds formed by a carboxyl group: the band significantly shifts to a low-wavenumber range of about 100 cm^{-1}, reaching a value of ∼1500 cm^{-1} at 2.69 GPa; at higher pressures, the band starts to overlap strongly with the others. The $(N-H)_{str}$ band preserves its narrow shape in the whole pressure range, indicating that an amide group is involved in only one hydrogen bond. This band shifts continuously to a low-wavenumber region of ∼80 cm^{-1} with increasing pressure and also with decreasing N···S distance in the corresponding N−H···S hydrogen bond (Figure 7a,b). The $(N-H)_{bend}$ and $(N-H)_{rock}$ gradually shift to a high-wavenumber region at ∼43 and 47 cm^{-1}, respectively, also confirming a significant strengthening of the N−H···S hydrogen bonds. The change in the S−H···O hydrogen bond is not simple: the $(S-H)_{str}$ band remains quite narrow and intensive without the formation of any shoulders that could point at the disorder of the thiol groups in the crystal. At the same time, its shift vs pressure is very interesting (Figure 7c,d). At the beginning, up to ∼1.5 GPa, the S···O2 distance shortening is accompanied by a decrease in the wavenumber of the $(S-H)_{str}$ band, which is in good agreement with the results obtained earlier.[28] This behavior corresponds to the strengthening of the S−H···O2 hydrogen bond in the crystal structure, though the D−H···A angle decreases. For a comparison, in both N−H···S and O−H···O hydrogen bonds, the D−H···A angle behaves "normally", i.e., slightly increases approaching the straight angle as the D···A distance decreases. Increasing pressure further still leads to a decrease in the S···O2 distance, but the corresponding $(S-H)_{str}$

dx.doi.org/10.1021/jp4068872 | J. Phys. Chem. B XXXX, XXX, XXX−XXX

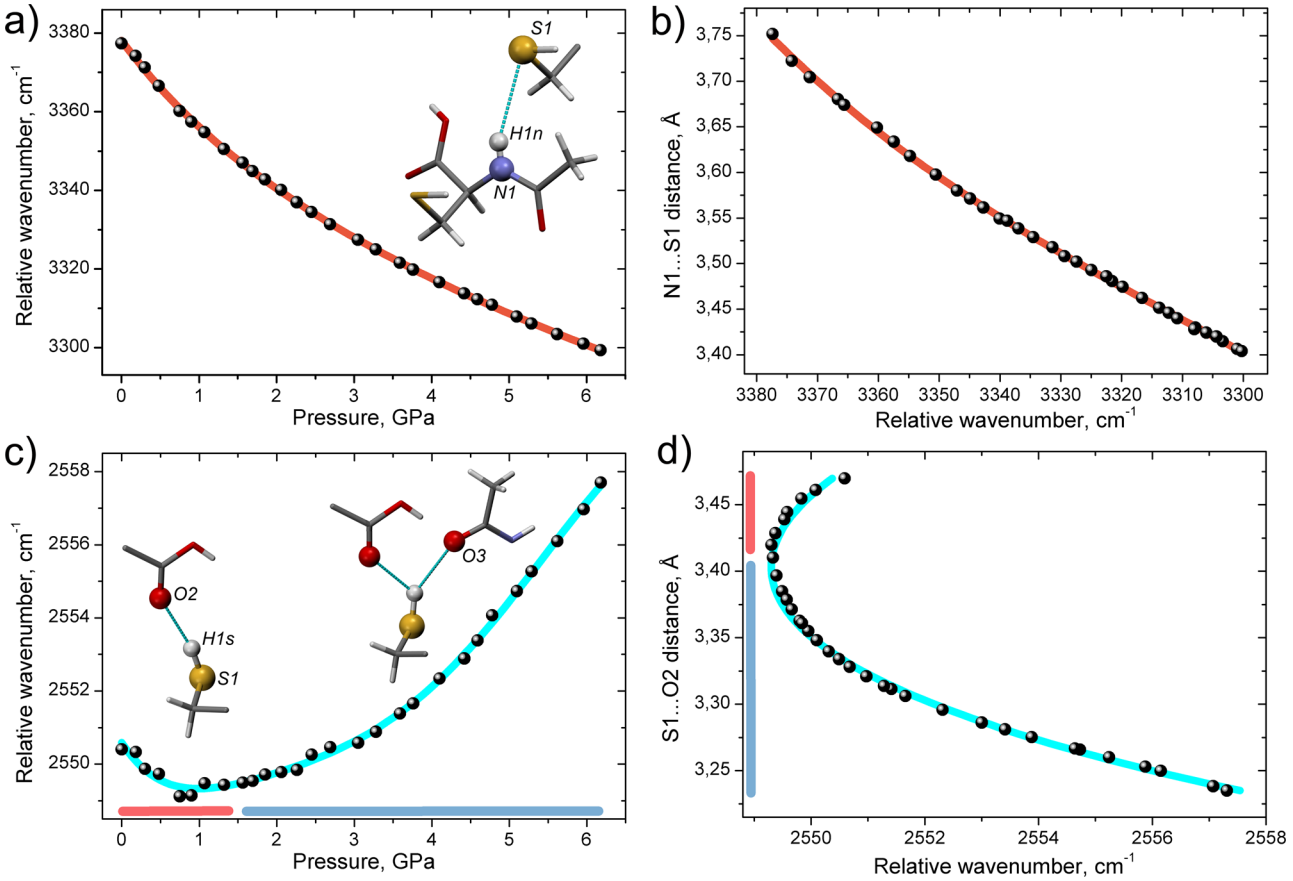

Figure 7. Pressure dependence of stretching vibrations of N−H and S−H groups (a and c, respectively). The shift of the wavenumber with changing D···A distance in the corresponding N1−H1n···S1 and S1−H1s···O2 hydrogen bonds (b and d, respectively). Each point in parts b and d corresponds to an experimental pressure point achieved in Raman or X-ray diffraction experiment, and the second coordinate is calculated from the fitting curve for the experimental data set. The curves are guides to the eye. The regions in which different hydrogen bonds contribute to the observed frequency shifts of the $(S-H)_{str}$ band are highlighted. For clarity, a schematic illustration of the hydrogen bonds is shown (the main part of a molecule is omitted for clarity).

band has a blue shift. This is caused by the formation of the three-centered S−H···O hydrogen bond: the thiol group starts to form additional S−H···O3 hydrogen bond with the carbonyl group of the neighboring molecule. Compression of the structure leads to a significant decrease in the S···O3 distance from 3.8885(8) Å at ambient pressure to 3.746(6) Å at 1.56 GPa and even to 3.546(5) Å at 6.05 GPa; the latter value corresponds to the geometrical parameters for a "statistically averaged" S−H···O hydrogen bond.[78] A simultaneous decrease in the S1−H1s···O2 angle and an increase in the S1−H1s···O3 angle with increasing pressure suggest that the proton migrates to form a three-centered hydrogen bond (Table 3). Even at the highest pressure achieved in the present experiment of 6.05 GPa, the S1−H1s···O2 and S1−H1s···O3 hydrogen bonds are not equivalent; therefore, a blue shift of the $(S-H)_{str}$ band is quite feasible. As the H1s proton moves, the short S1−H1s···O2 hydrogen bond weakens, whereas the longer S1−H1s···O3 bond becomes stronger. However, the S1···O3 distance is still longer as compared to S1···O2 distances, and therefore, its strengthening does not compensate for the weakening of the S1−H1s···O2 hydrogen bond.

A blue shift of the vibrational bands corresponding to the groups apparently involved in the bifurcated S−H···O hydrogen bond with increasing pressure was previously observed for orthorhombic L-cysteine.[58,59] We believe that increasing hydrostatic pressure results in formation of the bifurcated hydrogen bond in both phases: in the initial one (phase I, stable from ambient pressure to ∼2.5 GPa) and in the high-pressure phase appearing after the phase transition at ∼2.5 GPa (phase III). In phase I, increasing pressure leads to shortening of the S···O2 distance from 3.3788(15) Å at 10^{-4} GPa to 3.275(7) Å at 1.8 GPa accompanied by a blue shift of the $(S-H)_{str}$ band of about 29 cm^{-1} from ambient pressure to 2.04 GPa. Analysis of short contacts in phase I at 1.8 GPa revealed S···O1 equal to 3.501(7) Å (4.354(2) Å at 10^{-4} GPa), which should be considered as corresponding to a bifurcated S−H···O hydrogen bond. In phase III at 2.6 GPa, the thiol group should participate in the formation of a bifurcated hydrogen bond with a carboxylate group (with S···O1 and S···O2 distances of 3.432(7) and 3.713(8) Å, respectively), and not of a "common two-centered S···O1 hydrogen bond" as was defined by the authors of the original paper.[75] (Structural analysis of the L-cysteine phase III showed also the presence of another short S−H···O1 hydrogen bond (S···O1 distance of 3.375(8) Å, with a S−H···O1 angle of 106(4)°), but this H-bond was not taken into account because of its quite small S−H···O1 angle. Unfortunately, there are only few crystal structures of L-cysteine at high pressures, and for many of them, the thiol hydrogen is not located. Thus, in order to follow changes in the crystal structure on increasing pressure, more precise structural data are needed.) Further compression to 4.2 GPa leads to decrease of the S···O distances to 3.373(5) and 3.619(5) Å and to the

dx.doi.org/10.1021/jp4068872 | J. Phys. Chem. B XXXX, XXX, XXX−XXX

blue shift of the $(S-H)_{str}$ band from 2564 cm^{-1} (at 2.45 GPa) to 2571 cm^{-1} (at 3.9 GPa and even more, to 2584 cm^{-1} at 6.5 GPa), i.e., to the strengthening of the bifurcated S−H···O hydrogen bond. Although the accuracy in determination of S−H···O angles from the structural data obtained for the high-pressure phase of L-cysteine was low,[75] the tendency of their changes was similar to what was measured in this work for NAC.

The values characterizing the geometry of the O1−H1o···O3 hydrogen bond vs pressure are summarized in Table 3. The $(C{=}O)_{str}$ vibrations are very sensitive to the strengthening of this bond; a red shift of this band with pressure increasing up to 3.76 GPa indicates that the O1—H1o···O3 hydrogen bonds become stronger (Figure 8a). After this pressure is reached, the band maximum starts shifting in the opposite direction—to the higher wavenumbers. The situation is quite similar to the behavior of the $(S-H)_{str}$ band: at the beginning, the S1—H1s···O3 hydrogen bond is too weak to act as a competitor for the same O3 acceptor with a very strong O1—H1o···O3 hydrogen bond, and its influence on the shift of the $(C{=}O)_{str}$ band is negligible. However, at a certain pressure, the S1—H1s···O3 hydrogen bond starts to rival: at 4.42 GPa, the S1···O3 distance of 3.609(6) Å becomes comparable with the S···O distance in the low-temperature (or the first high-pressure) phase of DL-cysteine.[32,54] The $(S-H)_{bend}$ vibrations shift continuously to a high-wavenumber region at 25 cm^{-1}, the band maximum position reaching 1017 cm^{-1} at 6.18 GPa, without any hint of the pronounced effect observed for the $(S-H)_{str}$ vibrations. In ref 28, a non-monotonic shift of the $(S-H)_{str}$ band vs pressure was reported. The band maximum shifted in the higher-wavenumber region at pressures from ∼2 to ∼4 GPa, whereas increasing pressure further resulted in the opposite effect, namely, the "red" shift of this band, suggesting the strengthening of the S—H···O hydrogen bond. The discrepancy in the results obtained in two sets of experiments may be related to the usage of different pressure-transmitting fluids, one of which, fluorinert, is not absolutely hydrostatic, especially at very high pressures. Under non-hydrostatic conditions, different domains in the crystals can experience different pressure values. X-ray diffraction gives information averaged over the whole crystal, whereas Raman spectra are measured from a relatively small area in the crystal. It is technically impossible to measure Raman spectra at different pressures from the same area, and as a result, the measurements at different pressure values can correspond to different domains. This may be a reason why the previously published data obtained with a not completely hydrostatic medium were less accurate and precise.[28]

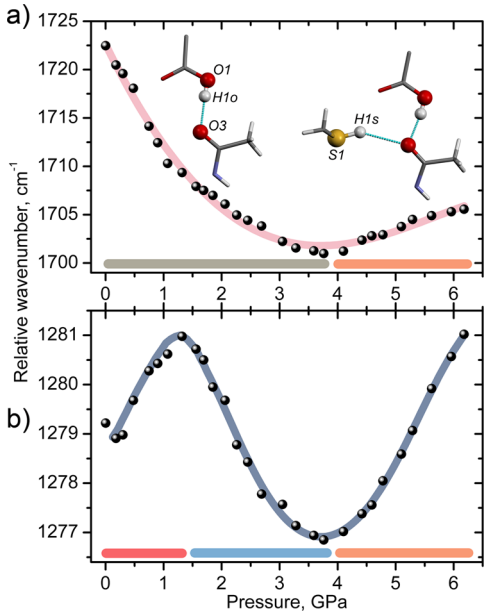

Figure 8. Pressure dependence of the stretching vibrations of the carbonyl C=O group (a) and wagging vibrations of the CH_2 group (b). The curves are guides to the eye. The regions in which different molecular fragments contribute to the shifts of the $(C{=}O)_{str}$ and $(CH_2)_{wagg}$ bands are highlighted. For clarity, schematic illustration of hydrogen bonds is shown (the main part of a molecule is omitted for clarity).

The band of the $(C-S)_{str}$ vibrations continuously shifted at about 44 cm^{-1} to the high-wavenumber region showing no hints of a jump-wise changing geometry of the $-CH_2-SH$ side chain during the formation of the bifurcated S−H···O hydrogen bond with increasing pressure, in contrast to what was observed during the pressure-induced phase transitions in orthorhombic L-cysteine and DL-cysteine.[58,59] The bands in the range of lattice vibrations significantly shifted to the high-wavenumber region, for example, no. 47–49 bands shifted at ∼50 cm^{-1} in agreement with a considerable compression of the crystal structure on increasing pressure.

All bands corresponding to the $(C-H)_{str}$ vibrations shifted to the higher wavenumbers with increasing pressure. The maximum change of about 70 cm^{-1} is observed for the no. 2 band. Thus, the C—H···S and C—H···O contacts observed in Hirshfeld's fingerprint plots are not really significant as interactions; otherwise, a red shift of the $(C-H)_{str}$ vibration would be detected. The no. 21 band characterizing the wagging vibrations of the CH_2 group changes continuously. For a comparison, on cooling of orthorhombic L-cysteine, the shift of this band had an S-shape dependence at about 150–200 K, indicating the jump-wise rotation of the $-CH_2-SH$ side chain of an amino acid during the ordering of thiol groups and switching from S—H···O to S—H···S hydrogen bonds.[60] In the Raman spectra of NAC on increasing pressure, $(CH_2)_{wagg}$ vibrations are also very sensitive to the changes related to the $-CH_2-SH$ side chain forming a bifurcated S—H···O hydrogen bond. In Figure 8b, one can distinguish three different regions divided by two extrema at about 1.3 and 3.8 GPa: the first region is related to the continuous shortening of S1···O2 distance in the S1—H1s···O2 hydrogen bond; the second one corresponds to the beginning of formation of the S1—H1s···O3 hydrogen bonds, i.e., to the changes related to a donor S—H group; and the last region describes the changes related to an acceptor C=O group, which begins to respond to the formation of a bifurcated S—H···O hydrogen bond later than a donor group, because of the presence of a stronger O1—H1o···O3 hydrogen bond. Thus, the mode of the $(CH_2)_{wagg}$ vibrations can act as some kind of a pressure-resolved indicator of the changes in the donor and the acceptor groups during the formation of the bifurcated hydrogen bond.

4. CONCLUSIONS

Summing up, although no phase transitions occur in NAC with increasing pressure and the changes in cell parameters and volume vs pressure do not reveal any peculiar features,[28] a more detailed analysis of the changes in the intermolecular distances,

dx.doi.org/10.1021/jp4068872 | J. Phys. Chem. B XXXX, XXX, XXX−XXX

in particular, of the geometric parameters of the hydrogen bonds based on X-ray single crystal diffraction analysis, complemented by an equally detailed study of the positions of all the significant bands in the Raman spectra, allowed us to study the fine details of subtle changes in the hydrogen-bond network, including the formation of the bifurcated hydrogen bonds.

The phase transitions observed for cysteine-containing crystals on increasing pressure and on cooling usually lead to the formation of stronger S−H···O hydrogen bonds in the crystal structure. The only known exception is orthorhombic L-cysteine: the thiol group, which is disordered between several positions at ambient conditions and can spontaneously form either S−H···O or S−H···S hydrogen bonds, gets ordered on cooling, preserving the S−H···S hydrogen bonds only.[31,60,79] In the crystal structure of NAC, the ordered S−H···O hydrogen bonds are formed at ambient temperature and pressure. Increasing pressure leads to gradual shifts of the thiol hydrogen, H1s, from O2 oxygen to O3, the way to form a three-centered bifurcated S−H···O hydrogen bond.

The results obtained in the present work allow us to suggest an interpretation of the data previously obtained for orthorhombic L-cysteine[58,59,75] and glutathione[80] in terms of the formation of the bifurcated S−H···O hydrogen bond. In the crystal of L-cysteine before the phase transition, increasing pressure results in formation of the three-centered hydrogen bond with considerable decrease of S···O1 distance and a large blue shift of the $(S-H)_{str}$ band. The first pressure-induced phase transition observed in orthorhombic L-cysteine at ∼2.5 GPa leads to a significant change in the side chain conformation and the formation of the S−H···O hydrogen bond with another O-atom acceptor as compared to ambient conditions. The authors defined this bond as a "common two-centered hydrogen bond",[75] though this bond might be classified as a three-centered one (S−H···O1 has the S···O1 distance of 3.432(7) Å and the S−H···O1 angle of 125(5)°, and the corresponding values for S−H···O2 are 3.713(8) Å and 138(5)°). Raman data showed that on increasing pressure further the $(S-H)_{str}$ band shifts from 2563 cm^{-1} at 2.5 GPa to 2584 cm^{-1} at 6.5 GPa, which was interpreted as weakening of the S−H···O1 hydrogen bond, though the S···O1 distance continued to decrease.[58,59] Although the S···O distance decreased in the two S−H···O hydrogen bonds (S···O1 and S···O2 became equal to 3.373(5) and 3.619(5) Å, respectively, at 4.2 GPa), the S−H···O angle had a tendency to decrease for the S−H···O1 hydrogen bond (120(4)°) and to increase for the S−H···O2 bond (145(4)°).[75] This situation is similar to what has been observed in this work for the NAC. Moreover, we believe that one can expect the continuous blue shift for the $(S-H)_{str}$ vibrations in the second high-pressure phase (formed at ∼3.7 GPa) of another cysteine-residue-containing compound, namely, glutathione, on increasing pressure further. The authors of ref 80 suggested the switching of the S−H···O hydrogen bond from one acceptor to another during the phase transition. However, this hydrogen bond could be considered as bifurcated again: the S···O1 and S···O2 distances are 3.691(5) and 3.261(8) Å, and the S−H···O1 and S−H···O2 angles are 151.6(1) and 153.0(1)°, respectively.

The gradual shift of the H1s hydrogen from a S1−H1s···O2 hydrogen bond to a S1−H1s···O3 bond forming a three-centered S−H···O hydrogen bond in the NAC with increasing pressure is related to the presence of the N−H···S hydrogen bond which tightly binds the $-CH_2-SH$ side chain and does not permit its free rotation, in contrast to relatively free thiol groups in L-cysteine, DL-cysteine, and glutathione which can easily change their conformation and switch over.

■ ASSOCIATED CONTENT

Supporting Information

Crystal structures of NAC at different pressures are presented as CIFs. This material is available free of charge via the Internet at http://pubs.acs.org. These crystal structures of NAC at different pressures are also deposited in the Cambridge Crystallographic Data Centre (CCDC No. 949292−949301); the data can be downloaded freely from the following site: http://www.ccdc.cam.ac.uk.

■ AUTHOR INFORMATION

Corresponding Authors

*E-mail: vasilyminkov@yahoo.com. Phone: +7-(383)-363-42-72.
*E-mail: eboldyreva@yahoo.com. Phone: +7-(383)-363-42-72.

Notes

The authors declare no competing financial interest.

■ ACKNOWLEDGMENTS

The authors acknowledge the financial support from the Ministry of Education and Science of the Russian Federation (Agreement No. 14.B37.21.1093) and the Integration Project No. 108 of the SB RAS.

■ REFERENCES

(1) Katrusiak, A. Macroscopic and Structural Effects of Hydrogen-Bond Transformations. *Crystallogr. Rev.* **1996**, *5*, 133−175.
(2) Katrusiak, A. Macroscopic and Structural Effects of Hydrogen-Bond Transformations. *Crystallogr. Rev.* **2003**, *9*, 91−133.
(3) Boldyreva, E. V. High-Pressure Studies of the Hydrogen Bond Networks in Molecular Crystals. *J. Mol. Struct.* **2003**, *700*, 151−155.
(4) Boldyreva, E. V. High-Pressure Diffraction Studies of Molecular Organic Solids. A Personal View. *Acta Crystallogr., Sect. A* **2007**, *64*, 218−231.
(5) Sikka, S. K.; Sharma, S. M. The Hydrogen Bond Under Pressure. *Phase Transitions* **2008**, *81*, 907−934.
(6) Boldyreva, E. V. Combined X-ray Diffraction and Raman Spectroscopy Studies of Phase Transitions in Crystalline Amino Acids at Low Temperatures and High Pressures: Selected Examples. *Phase Transitions* **2009**, *82*, 303−321.
(7) Boldyreva, E. V. High-Pressure Studies of the Anisotropy of Structural Distortion of Molecular Crystals. *J. Mol. Struct.* **2003**, *647*, 159−179.
(8) Boldyreva, E. V. High-Pressure-Induced Structural Changes in Molecular Crystals Preserving the Space Group Symmetry: Anisotropic Distortion/Isosymmetric Polymorphism. *Cryst. Eng.* **2003**, *6*, 235−254.
(9) Boldyreva, E. V. Supramolecular Systems Under Extreme Conditions. *Herald Russ. Acad. Sci.* **2012**, *82*, 423−431.
(10) Kumar, S. S.; Nangia, A. A New Conformational Polymorph of N-Acetyl-L-Cysteine. The Role of S−H···O and C−H···O Interactions. *CrystEngComm* **2013**, *15*, 6498−6505.
(11) Smilkstein, M.; Knapp, G.; Kulig, K.; Rumack, B. Efficacy of Oral N-Acetylcysteine in the Treatment of Acetaminophen Overdose. *New Engl. J. Med.* **1988**, *319*, 1557−1562.
(12) Gibson, K. R.; Neilson, I. L.; Barrett, F.; Winterburn, T. J.; Sharma, S.; MacRury, S. M.; Megson, I. L. Evaluation of the Antioxidant Properties of N-Acetylcysteine in Human Platelets: Prerequisite for Bioconversion to Glutathione for Antioxidant and Antiplatelet Activity. *J. Cardiovasc. Pharmacol.* **2009**, *54*, 319−326.
(13) Heard, K.; Green, J. Acetylcysteine Therapy for Acetaminophen Poisoning. *Curr. Pharm. Biotechnol.* **2012**, *13*, 1917−1923.

(14) Dean, O.; Giorlando, F.; Berk, M. N-Acetylcysteine in Psychiatry: Current Therapeutic Evidence and Potential Mechanisms of Action. *J. Psychiatry Neurosci.* **2011**, *36*, 78−86.
(15) Sansone, R. A.; Sansone, L. A. Faking Attention Deficit Hyperactivity Disorder. *Innov. Clin. Neurosci.* **2011**, *8*, 10−13.
(16) Ippolito, J. A.; Alexander, R. S.; Christianson, D. W. Hydrogen Bond Stereochemistry in Protein Structure and Function. *J. Mol. Biol.* **1990**, *215*, 457−471.
(17) Gregoret, L. M.; Rader, S. D.; Fletterick, R. J.; Cohen, F. E. Hydrogen Bonds Involving Sulfur Atoms in Proteins. *Proteins* **1991**, *9*, 99−107.
(18) Pal, D.; Chakrabarti, P. Different Types of Interactions Involving Cysteine Sulfhydryl Group in Proteins. *J. Biomol. Struct. Dyn.* **1998**, *15*, 1059−1072.
(19) Rajagopal, S.; Vishveshwara, S. Short Hydrogen Bonds in Proteins. *FEBS J.* **2005**, *272*, 1819−1832.
(20) Panigrahi, S. K.; Desiraju, G. R. Strong and Weak Hydrogen Bonds in the Protein-Ligand Interface. *Proteins* **2007**, *67*, 128−141.
(21) Zhou, P.; Tian, F.; Lv, F.; Shang, Z. Geometric Characteristics of Hydrogen Bonds Involving Sulfur Atoms in Proteins. *Proteins* **2009**, *76*, 151−163.
(22) Rebar, E. J.; Pabo, C. O. Zinc Finger Phage: Affinity Selection of Fingers With New DNA-Binding Specificities. *Science* **1994**, *263*, 671−673.
(23) Beinert, H.; Kiley, P. J. Fe-S in Sensing and Regulatory Functions. *Curr. Opin. Chem. Biol.* **1999**, *3*, 152−157.
(24) Beinert, H. Iron-Sulfur Proteins: Ancient Structures, Still Full of Surprises. *J. Biol. Inorg. Chem.* **2000**, *5*, 2−15.
(25) Krishna, S. S.; Majumdar, I.; Grishin, N. V. Structural Classification of Zinc Fingers. *Nucleic Acids Res.* **2003**, *31*, 532−550.
(26) Johnson, D. C.; Dean, D. R.; Smith, A. D.; Johnson, M. K. Structure, Functions, and Formation of Biological Iron-Sulfur Clusters. *Annu. Rev. Biochem.* **2005**, *74*, 247−281.
(27) Lill, R.; Muhlenhoff, U. Iron-Sulfur-Protein Biogenesis in Eukaryotes. *Trends Biochem. Sci.* **2005**, *30*, 133−141.
(28) Minkov, V. S.; Boldyreva, E. V.; Drebushchak, T. N.; Görbitz, C. H. Stabilizing Structures of Cysteine-Containing Crystals with Respect to Variations of Temperature and Pressure by Immobilizing Amino Acid Side Chains. *CrystEngComm* **2012**, *14*, 5943−5954.
(29) Kolesov, B. A.; Boldyreva, E. V. Difference in the Dynamic Properties of Chiral and Racemic Crystals of Serine Studied by Raman Spectroscopy at 3−295 K. *J. Phys. Chem. B* **2007**, *111*, 14387−14397.
(30) Minkov, V. S.; Chesalov, Yu. A.; Boldyreva, E. V. A Study of the Temperature Effect on the IR Spectra of Crystalline Amino Acids, Dipeptids, and Polyamino Acids. VI. L-Alanine and DL-Alanine. *J. Struct. Chem.* **2010**, *51*, 1052−1063.
(31) Kolesov, B. A.; Minkov, V. S.; Boldyreva, E. V.; Drebushchak, T. N. Phase Transitions in the Crystals of L- and DL-Cysteine on Cooling: the Role of the Hydrogen-Bond Distortions and the Side-Chain Motions of Thiol-Groups. 1. L-Cysteine. *J. Phys. Chem. B* **2008**, *112*, 12827−12839.
(32) Minkov, V. S.; Tumanov, N. A.; Kolesov, B. A.; Boldyreva, E. V.; Bizyaev, S. N. Phase Transitions in the Crystals of L- and DL-Cysteine on Cooling: Intermolecular Hydrogen Bonds Distortions and the Side-Chain Motions of Thiol-Groups. 2. DL-Cysteine. *J. Phys. Chem. B* **2009**, *113*, 5262−5272.
(33) Zakharov, B. A.; Kolesov, B. A.; Boldyreva, E. V. Monitoring Selected Hydrogen Bonds in Crystal Hydrates of Amino Acid Salts: Combining Variable-Temperature Single-Crystal X-ray Diffraction and Polarized Raman Spectroscopy. *Phys. Chem. Chem. Phys.* **2011**, *13*, 13106−13116.
(34) Zakharov, B. A.; Boldyreva, E. V. A High-Pressure Single-Crystal to Single-Crystal Phase Transition in DL-Alaninium Semi-Oxalate Monohydrate with Switching-Over Hydrogen Bonds. *Acta Crystallogr., Sect. B* **2013**, *69*, 271−280.
(35) Li, Q.; Li, S.; Wang, K.; Li, X.; Liu, J.; Liu, B.; Zou, G.; Zou, B. Pressure-Induced Isosymmetric Phase Transition in Sulfamic Acid: A Combined Raman and X-ray Diffraction Study. *J. Chem. Phys.* **2013**, *138*, 214303-1−214303-8.
(36) Piermarini, G. J.; Block, S.; Barnett, J. D.; Forman, R. A. Calibration of the Pressure Dependence of the R1 Ruby Fluorescence Line to 195 kbar. *J. Appl. Phys.* **1975**, *46*, 2774−2780.
(37) *CrysAlis CCD and CrysAlis RED*; Oxford Diffraction Ltd: Abingdon, England, 2008.
(38) Angel, R. J. Absorption Corrections for Diamond-Anvil Pressure Cells Implemented in the Software Package - Absorb6.0. *J. Appl. Crystallogr.* **2004**, *37*, 486−492.
(39) Sheldrick, G. M. *Program for Refinement of Crystal Structures*; University of Göttingen: Göttingen, Germany, 1997.
(40) Sheldrick, G. M. A Short History of SHELX. *Acta Crystallogr., Sect. A* **2008**, *64*, 112−122.
(41) *X-STEP32*; STOE & Cie GmbH: Darmstadt, Germany, 2000.
(42) Dolomanov, O. V.; Bourhis, L. J.; Gildea, R. J.; Howard, J. A. K.; Puschmann, H. OLEX2: a Complete Structure Solution, Refinement and Analysis Program. *J. Appl. Crystallogr.* **2009**, *42*, 339−341.
(43) Macrae, C. F.; Edgington, P. R.; McCabe, P.; Pidcock, E.; Shields, G. P.; Taylor, R.; Towler, M.; Streek, J. van de. Mercury: Visualization and Analysis of Crystal Structures. *J. Appl. Crystallogr.* **2006**, *39*, 453−457.
(44) McKinnon, J. J.; Spackman, M. A.; Mitchell, A. S. Novel Tools for Visualizing and Exploring Intermolecular Interactions in Molecular Crystals. *Acta Crystallogr., Sect. B* **2004**, *60*, 627−668.
(45) McKinnon, J. J.; Jayatilaka, D.; Spackman, M. A. Towards Quantitative Analysis of Intermolecular Interactions with Hirshfeld Surfaces. *Chem. Commun.* **2007**, *37*, 3814−3816.
(46) Spek, A. L. Single-Crystal Structure Validation with the Program PLATON. *J. Appl. Crystallogr.* **2003**, *36*, 7−13.
(47) Cliffe, M. J.; Goodwin, A. L. PASCal: a Principal Axis Strain Calculator for Thermal Expansion and Compressibility Determination. *J. Appl. Crystallogr.* **2012**, *45*, 1321−1329.
(48) Takusagawa, F.; Koetzle, T. F.; Kou, W. W. H.; Parthasarathy, R. Structure of N-Acetyl-L-Cysteine: X-ray (T=295 K) and Neutron (T=16 K) Diffraction Studies. *Acta Crystallogr., Sect. B* **1981**, *37*, 1591−1596.
(49) Kerr, K. A.; Ashmore, J. P. Structure and Conformation of Orthorhombic L-Cysteine. *Acta Crystallogr., Sect. B* **1973**, *29*, 2124−2127.
(50) Kerr, K. A.; Ashmore, J. P.; Koetzle, F. A Neutron Diffraction Study of L-Cysteine. *Acta Crystallogr., Sect. B* **1975**, *31*, 2022−2026.
(51) Boldyreva, E. V. Crystalline Amino Acids - a Link Between Chemistry, Materials Science and Biology. In *Models, Mysteries, and Magic of Molecules*; Boeyens, J. C. A., Ogilvie, J. F., Eds.; Springer: Berlin, 2007; p 169.
(52) Etter, M. C.; MacDonald, J. C.; Bernstein, J. Graph-Set Analysis of Hydrogen-Bond Patterns in Organic-Crystals. *Acta Crystallogr., Sect. B* **1990**, *46*, 256−262.
(53) Görbitz, C. H.; Dalhus, B. L-Cysteine, Monoclinic Form, Redetermination at 120 K. *Acta Crystallogr., Sect. C* **1996**, *52*, 1756−1759.
(54) Minkov, V. S.; Tumanov, N. A.; Boldyreva, E. V.; Cabrera, R. Q. Low Temperature/High Pressure Polymorphism in DL-Cysteine. *CrystEngComm* **2010**, *12*, 2551−2560.
(55) Allen, F. H. The Cambridge Structural Database: a Quarter of a Million Crystal Structures and Rising. *Acta Crystallogr., Sect. B* **2002**, *58*, 380−388.
(56) Suresh, S. G.; Vijayan, M. Occurrence and Geometrical Features of Head-to-Tail Sequences Involving Amino-Acids in Crystal-Structures. *Int. J. Pept. Protein Res.* **1983**, *22*, 129−143.
(57) Bondi, A. Van der Waals Volumes and Radii. *J. Phys. Chem.* **1964**, *68*, 441−451.
(58) Minkov, V. S.; Goryainov, S. V.; Boldyreva, E. V.; Görbitz, C. H. Raman Study of Pressure-Induced Phase Transitions in Crystals of Orthorhombic and Monoclinic Polymorphs of L-Cysteine: Dynamics of the Side Chain. *J. Raman Spectrosc.* **2010**, *41*, 1748−1758.
(59) Minkov, V. S.; Krylov, A. S.; Boldyreva, E. V.; Goryainov, S. V.; Bizyaev, S. N.; Vtyurin, A. N. Pressure-Induced Phase Transitions in Crystalline L- and DL-Cysteine. *J. Phys. Chem. B* **2008**, *112*, 8851−8854.

(60) Min'kov, V. S.; Chesalov, Yu. A.; Boldyreva, E. V. Study of the Temperature Effect on IR Spectra of Crystalline Amino Acids, Dipeptides, and Polyamino Acids. IV. L-Cysteine and DL-Cysteine. *J. Struct. Chem.* **2008**, *49*, 1022−1034.
(61) Novak, A. Hydrogen Bonding in Solids. Correlation of Spectroscopic and Crystallographic Data. *Struct. Bonding (Berlin, Ger.)* **1974**, *18*, 177−216.
(62) Susi, H.; Byler, D. M.; Gerasimowicz, W. V. Vibrational Analysis of Amino Acids: Cysteine, Serine, *β*-Chloroalanine. *J. Mol. Struct.* **1983**, *102*, 63−79.
(63) Tarakeshwar, P.; Manogaran, S. Vibrational Frequencies of Cysteine and Serine Zwitterions - an *ab initio* Assignment. *Spectrochim. Acta, Part A* **1995**, *51*, 925−928.
(64) Chakraborty, D.; Manogaran, S. Ground State Vibrational Spectra of Cysteine and Serine Zwitterion: a Theoretical Prediction. *J. Mol. Struct.: THEOCHEM* **1998**, *429*, 31−40.
(65) Pawlukojc, A.; Leciejewicz, J.; Ramirez-Cuesta, A. J.; Nowicka-Scheibe, J. L-Cysteine: Neutron Spectroscopy, Raman, IR and *ab initio* Study. *Spectrochim. Acta, Part A* **2005**, *61*, 2474−2481.
(66) Wolpert, M.; Hellwig, P. Infrared Spectra and Molar Absorption Coefficients of the 20 Alpha Amino Acids in Aqueous Solutions in the Spectral Range From 1800 to 500 cm^{-1}. *Spectrochim. Acta, Part A* **2006**, *64*, 987−1001.
(67) Rungsawang, R.; Ueno, Y.; Tomita, I.; Ajito, K. Angle-Dependent Terahertz Time-Domain Spectroscopy of Amino Acid Single Crystals. *J. Phys. Chem. B* **2006**, *110*, 21259−21263.
(68) Guicheteau, J.; Argue, L.; Hyre, A.; Jacobson, M.; Christesen, S. D. Raman and Surface-Enhanced Raman Spectroscopy of Amino Acids and Nucleotide Bases for Target Bacterial Vibrational Mode Identification. *Proc. SPIE* **2006**, *6218*, Art. No. 62180O.
(69) Korter, T. M.; Balu, R.; Campbell, M. B.; Beard, M. C.; Gregurick, S. K.; Heilweil, E. Terahertz Spectroscopy of Solid Serine and Cysteine. *J. Chem. Phys. Lett.* **2006**, *418*, 65−70.
(70) Dobrowolski, J. C.; Jamroz, M. H.; Kolos, R.; Rode, J. E.; Sadlej, J. Theoretical Prediction and the First IR Matrix Observation of Several L-Cysteine Molecule Conformers. *ChemPhysChem* **2007**, *8*, 1085−1094.
(71) Bellamy, L. J. *The Infrared Spectra of Complex Molecules*, 3rd ed.; Halsted Press, a division of John Wiley & Sons, Inc.: New York, 1975; Vol. 1, p 433.
(72) Zhao, J.; Angel, R. J.; Ross, N. L. Effects of deviatoric stresses in the diamond-anvil pressure cell on single-crystal samples. *J. Appl. Crystallogr.* **2010**, *43*, 743−751.
(73) Boldyreva, E. V.; Ahsbahs, H.; Uchtmann, H.; Kashcheeva, N. E. Effects of Pressure on the Two Polymorphs of $[Co(NH_3)_5NO_2]I_2$: The Anisotropy of Lattice Distortion and a Phase Transition. *High Pressure Res.* **2000**, *17*, 79−99.
(74) Boldyreva, E. V.; Dmitriev, V.; Hancock, B. C. Effect of Pressure up to 5.5 GPa on Dry Powder Samples of Chlorpropamide Form-A. *Int. J. Pharm.* **2006**, *327*, 51−57.
(75) Moggach, S. A.; Allan, D. R.; Clark, S. J.; Gutmann, M. J.; Parsons, S.; Pulham, C. R.; Sawyer, L. High-Pressure Polymorphism in L-Cysteine: the Crystal Structures of L-Cysteine-III and L-Cysteine-IV. *Acta Crystallogr., Sect. B* **2006**, *62*, 296−309.
(76) Seryotkin, Yu. V.; Drebushchak, T. N.; Boldyreva, E. V. A High-Pressure Polymorph of Chlorpropamide Formed on Hydrostatic Compression of the Alpha-Form in Saturated Ethanol Solution. *Acta Crystallogr., Sect. B* **2013**, *69*, 77−85.
(77) Spackman, M. A.; McKinnon, J. J. Fingerprinting Intermolecular Interactions in Molecular Crystals. *CrystEngComm* **2002**, *4*, 378−392.
(78) Desiraju, G. R.; Steiner, T. *Weak Hydrogen Bond: In Structural Chemistry and Biology*; Oxford University Press: 1991; p 569.
(79) Moggach, S. A.; Clark, S. J.; Parsons, S. L-Cysteine-I at 30 K. *Acta Crystallogr., Sect. E* **2005**, *61*, o2739−o2742.
(80) Moggach, S. A.; Lennie, A. R.; Morrison, C. A.; Richardson, P.; Stefanowicz, F. A.; Warren, J. E. Pressure Induced Phase Transitions in the Tripeptide Glutathione to 5.24 GPa: the Crystal Structure of Glutathione-II at 2.94 GPa and Glutathione-III at 3.70 GPa. *CrystEngComm* **2010**, *12*, 2587−2595.